Parameters Influencing the Generation of the L, S, and C-bands (1 – 8 GHz) Emission from Hall Thrusters

IEPC-2009-072

Edward J. Beiting, Rostislav Spektor, and Xuan Le Eapen
The Aerospace Corporation
P.O. Box 92957 – M2/341
Los Angeles, CA 90009-2957

A parametric study on the origins of the 1 – 8 GHz emission radiated from Hall Current Thrusters (HCTs) was undertaken. The effect of cathode angle, discharge voltage, cathode flow rate, and magnetic field were investigated by observing the emission from the thruster using MIL-STD 461E RE102 specifications in The Aerospace Corporation electric propulsion EMC facility. Measurements were made on a 2 kW class laboratory Hall thruster equipped with Heatwave hollow cathode. The thruster operated at powers between 180 and 1120 W. These studies indicate that changes in cathode angle do not significantly alter the radiated electric field in the L, S, and C-bands. The same is true for variations in the cathode flow rate with the exception of the L-band emission being sensitive the cathode operating in a xenon starved condition. When the magnetic field is held constant, there is an inverse relationship between emission and discharge voltage: a higher voltage producing a lower emission across all three bands. The emission in these bands proves to be sensitive to changes in magnetic field; increasing the magnetic field increases the emission. Time domain measurements made in the 1-3 GHz frequency range using a digital oscilloscope revealed that emission is pulsed. Characteristics of the pulse amplitude, width, and frequency are presented.

Nomenclature

sccm	=	flow rate in standard cubic centimeters per minute
DSO	=	digital sampling oscilloscope
EMC	=	electromagnetic compatibility
HCT	=	Hall current thruster
LNA	=	low noise amplifier
LSC	=	1 – 8 GHz bands
MIL-STD	=	Military Standard
RF	=	radio frequency

I. Introduction

Before an electric thruster can be integrated onto a satellite bus, a characterization of its radiated emission is required. Numerous studies have shown that Hall thrusters produce strong emission from DC to well into the K-band (> 18 GHz). Emission below a few hundred MHz has been associated with various plasma modes[1] whereas emission above 18 GHz is due to the electron plasma frequency radiation.[2] The origin of the strong emission in the L, S and C-bands (1 – 8 GHz), however, is largely unknown although it has been addressed in several studies.[3-5] This emission can reduce the sensitivity of on-board receivers and there is some evidence that the strength of this emission may increase significantly as the thruster ages for the SPT-100 thruster. [3,6] A study of this emission in the time domain has found it to be pulsed with envelope pulse lengths varying by from tens of nanoseconds to a few microseconds.[7]

A recent study of this LSC emission at The Aerospace Corporation using antennas and a specially designed high frequency probe found that the L-band (1-2 GHz) radiation is associated with the cathode whereas the S- and C-band emission is more complex and associated with the thruster plume or an interaction of the cathode plume with the thruster main plume.[8] More recent studies discovered that this LSC emission from two very similar commercial Hall thrusters (the PPS®1350 and the SPT-100) is markedly different.[9] It is this recent observation that, in part, motivates the work presented in this paper.

We present both spectral and time domain data studying this emission. As part of this work, we endeavor to understand which thruster parameters most influence the strength of this radiation. We present data that explores the influence of cathode angle, magnetic field, discharge voltage, and cathode flow rate. Additionally, we characterized the pulsed nature of the emission by measuring the frequency, amplitude, and envelope pulse width of each individual pulse. This paper is divided into four sections: Section II presents a brief description of the facility and thruster, Section III presents the results of the measurements, and Section IV summarizes the findings and draws some conclusions.

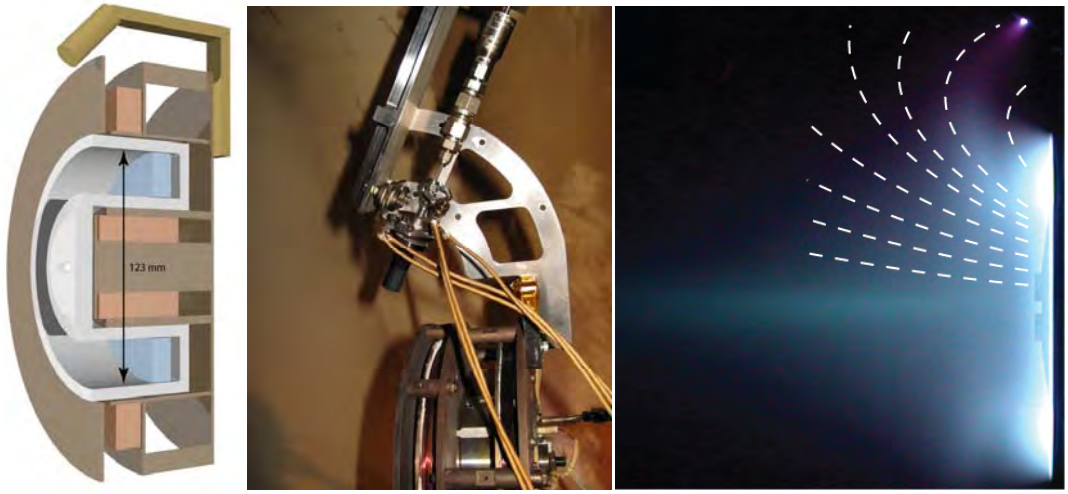

Figure 1. Three views of the GPT-1 Hall Thruster. (a) Left panel is a schematic of the thruster showing the inner and outer magnets (copper color), boron nitride channel (white), anode (blue), and cathode at top. (b) Center panel is a photograph of the cathode on the fixture used to adjust the cathode angle with respect to the thruster axis. (c) Right panel is a picture of the GPT-1thruster in operation where typical measured magnetic field lines are shown; the bright spot at the top right of this photo is the cathode orifice.

II. Facility and Thruster

All work was carried out at the recently upgraded The Aerospace Corporation's electric propulsion EMC facility; it is described and characterized elsewhere.[10] For convenience, we note here that the facility comprises a 1 m diameter by 1.5 m long cylindrical dielectric tank surrounded by a semi-anechoic room. The thruster, located inside the dielectric tank, exhausts into a 2.4 m diameter by 10 m long vacuum chamber. Antennas used to sense the radiation are placed outside the dielectric tank 1 m from the thruster; instrumentation is located outside the anechoic room. Pressure in the tank during measurement varied between 0.3–1.0 x 10^{-5} mbar (corrected) depending on the xenon flow rate.

Figure 1 presents three views of the 2 kW-class Hall thruster used. The thruster, developed by General Plasma Technology Inc., consists of a 4.2 cm long and 2.5 cm wide boron nitride annular channel with inner diameter of 7.3 cm. The same material is used to cap the center section of the thruster. Two independent magnet coils, shown in Fig. 1(a) with copper color, create a mostly radial magnetic field in the thruster channel. The thruster uses a standard Heatwave HWPES-250 hollow cathode. This thruster is similar in design and operation to the thruster investigated by Raitses *et al.*[11,12]

Table I lists some of the operating modes of the thruster used for this work. This selection permitted the exploration emission over the parameter space. The cathode was operated in a xenon starved condition in modes 1-3 and 13-15. Spectra were acquired for three cathode angles (0^o, 30^o, and 60^o) for each of modes 1-24. The magnetic field in the first 12 modes were chosen to minimize the discharge current and discharge current oscillations for a given discharge voltage and flow rate, a common method used for choosing a stable operating point for a Hall thruster. The magnetic field settings in modes 13-24 were held constant while the discharge potential was varied. The anode flow rate was 19 sccm for the first 12 modes and almost twice this value (35 sccm) for the second 12 modes. The modes 25-29 (below the dashed line) were used to explore the effect of changing the magnetic field gradient on the LSC emission while holding all other parameters constant. These magnetic fields were chosen to bracket the fields used in the first 24 modes.

Table 1

Mode	Flow Rate Anode (sccm)	Flow Rate Cathode (sccm)	Discharge Potential (V)	Magnet Current Inner (A)	Magnet Current Outer (A)	Discharge Current (A)	Power (W)	Remark
1	19	0.95	150	0.60	0.77	1.2	180	1
2	19	0.95	250	0.70	1.13	1.5	370	1
3	19	0.95	350	0.90	1.21	1.7	595	1
4	19	1.425	150	0.60	0.77	1.2	180	1
5	19	1.425	250	0.70	1.13	1.5	380	1
6	19	1.425	350	0.90	1.21	1.7	592	1
7	19	1.9	150	0.60	0.77	1.2	180	1
8	19	1.9	250	0.70	1.13	1.5	380	1
9	19	1.9	350	0.90	1.21	1.7	595	1
10	19	2.85	150	0.60	0.77	1.2	180	1
11	19	2.85	250	0.70	1.13	1.5	380	1
12	19	2.85	350	0.90	1.21	1.7	581	1
13	35	1.75	150	0.80	1.3	3.1	458	2
14	35	1.75	250	0.80	1.3	3.0	745	2
15	35	1.75	350	0.80	1.3	3.2	1103	2
16	35	2.625	150	0.80	1.3	3.1	461	2
17	35	2.625	250	0.80	1.3	3.0	743	2
18	35	2.625	350	0.80	1.3	3.1	1085	2
19	35	3.5	150	0.80	1.3	3.1	462	2
20	35	3.5	250	0.80	1.3	3.0	750	2
21	35	3.5	350	0.80	1.3	3.1	1085	2
22	35	5.25	150	0.80	1.3	3.1	465	2
23	35	5.25	250	0.80	1.3	3.0	750	2
24	35	5.25	350	0.80	1.3	3.2	1120	2
25	19	1.9	350	0.80	0.8	1.7	609	3
26	19	1.9	350	0.80	1.1	1.6	574	3,4
27	19	1.9	350	0.80	1.4	1.7	606	3
28	19	1.9	350	0.56	1.1	1.8	623	3
29	19	1.9	350	1.04	1.1	1.8	630	3

Remarks: 1 = magnet current set for minimum anode current and oscillation; 2 = magnet currents not varied; 3 = magnetic field study; 4 = nominal set point for anode flow of 19 sccm and 350V.

III. Measurements and Data

As noted above, spectral and time domain measurements were made. The spectral measurements, which are useful to gain an overview of the emission from the thruster, are presented first. However, most of the emission in the L-, S-, and C-bands (1-8 GHz) is pulsed and viewing only spectra can give misleading impressions of the relative importance of the emission in these bands. Spectra presented in this section were acquired using a well-characterized double ridge horn antenna connected through an external low noise amplifier to a calibrated Rohde & Schwarz ESIB 26 EMI test receiver and followed MIL-STD 461E RE102 specifications. Software written in-house controlled both this instrumentation and the processing of the data.

One of the principal differences between the SPT-100 and the PPS-1350 thrusters is the cathode angle with respect to the thruster axis.[13] This parameter was investigated by mounting the cathode on a fixture that permitted the cathode angle to be adjusted to values of 0^o, 30^o, 45^o, and 60^o with respect to the thruster axis while maintaining the same position of the cathode exit orifice (see Figure 1b). Spectral scans were taken for all discharge potentials, cathode and anode flow rates (thruster modes 1-24) at 0^o, 30^o, and 60^o. A representative example of these data is shown in Figure 2 for a discharge potential of 250 V. We observed no significant difference among the spectra for these three angles for the first 24 different operating conditions listed in Table 1. Accordingly, we conclude that LSC emission is not dependent on cathode angle.

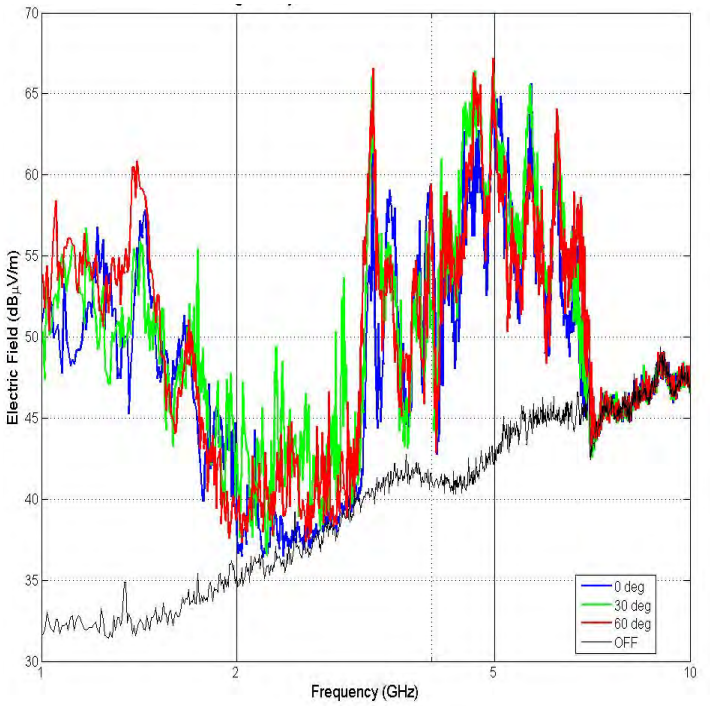

Figure 2. LSC spectra as a function of cathode angle for thruster mode 8.

Figures 3 and 4 both show four panels of three spectra each. Figure 3 shows the thruster operating at low power with an anode flow rate of 35 sccm whereas Figure 4 shows a similar set of data with the thruster operating at about half the power with an anode flow rate of 19 sccm. The data in each panel were taken with the same cathode flow rate and the spectra within a panel were taken with different discharge potentials. A significant difference Figures 3 and 4 is the magnetic field. In Figure 3 the magnetic field was held constant throughout (modes 13-24) whereas in Figure 4 the magnetic field was varied with discharge potential to minimize the anode current oscillations and hence is more what one would expect for normal thruster operation (modes 1-12). The cathode flow rate was chosen so that ratio of the cathode flow to anode flow was the same for corresponding panels in Figure 3 and 4.

First, we examine Figure 3 where the magnetic field is constant for all scans. Here we note that there is no statistically significant difference among the spectra with increasing cathode flow rate for the lower two discharge voltages. Indeed, the emission is nearly identical for the discharge voltages of 150V and 250V with the exception of the higher emission between 4-5 GHz for the lowest voltage (150V). Interestingly, the emission is lowest for all frequencies and scans for the highest discharge voltage (350V) and this is especially true for the L-band with the thruster operating with the cathode "xenon starved" with a flow of 1.75 sccm. With a cathode flow increased to $\geq$ 2.6 sccm the L-band emission increases (nearly 20 dB at 1.5 GHz) and the S- and C-band emission nearly drop to background levels for the at 350V case. In general the 350V emission never exceeds the level of the 150V and 250 V emission levels. From these data we conclude that unless the cathode is xenon starved, emission in the LSC bands is not strongly dependent on cathode flow rate and decreases with an increase in the discharge voltage across all three bands.

Now examine Figure 4 where the magnetic field was adjusted with discharge voltage within each panel to yield the most stable thruster operation. Here we first note that the variation of emission as a function of discharge voltage is much larger than that seen in Figure 3. Furthermore, in the contrast with the constant magnetic field case, the highest discharge voltage results in the highest emission in all three bands. We also note that for the highest discharge voltage the L-band emission is highest with the cathode operating in the "xenon starved" mode. Similar to constant magnetic field case, we see little change in emission with cathode flow rate with the exception of the "xenon starved" L-band emission. There does appear to be significant change in emission with discharge voltage. Based on the data of Figure 4, however, we tentatively draw the conclusion that this change in emission is likely due to the change in magnetic field, which was altered with the discharge voltage.

Because of the many changing parameters, a comparison of spectra in Figures 3 and 4 does not allow us to draw solid conclusions about the variation of emission with varying anode flow rate. Interestingly, however, for the 350V discharge potential the emission is greater for the low anode flow (lower power) operation and lower for the higher anode flow rate (higher power) operation. This inverse relationship again implicates the magnetic field as the significant parameter.

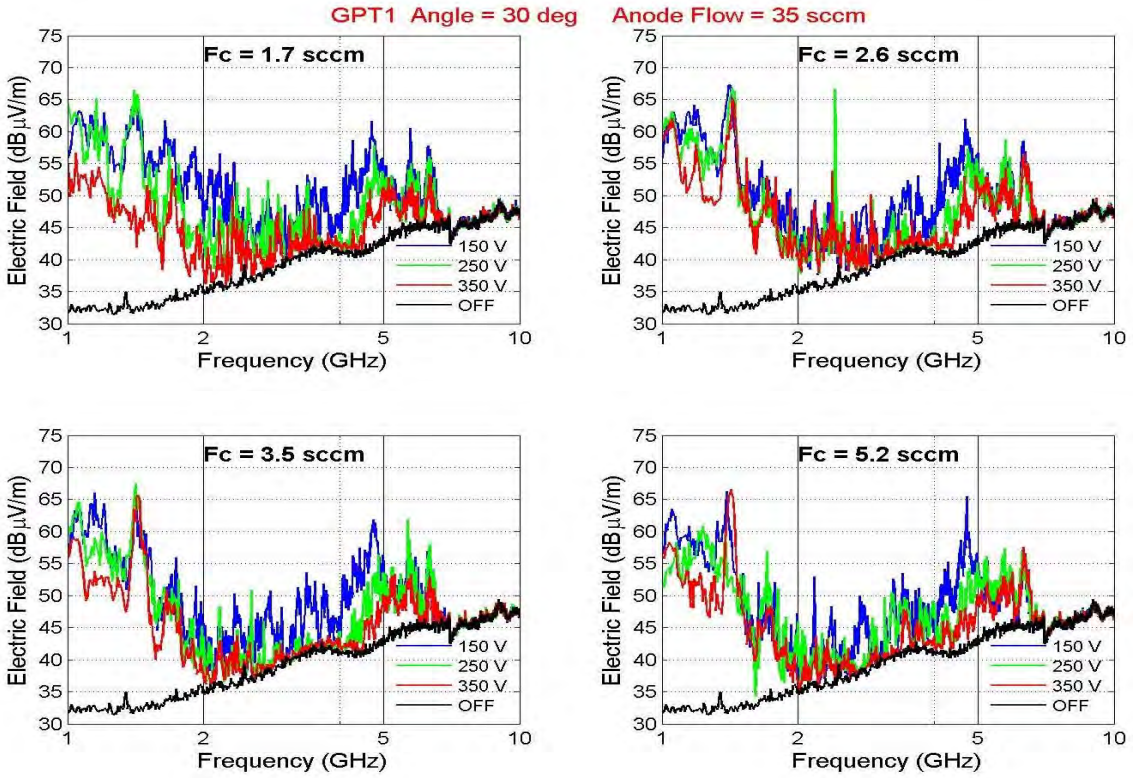

Figure 3. 1-10 GHz emission for an anode flow rate of 35 sccm, 4 cathode flow rates, and 3 discharge voltages. Magnetic field is the same for all spectra. The black line is the background emission (thruster unpowered).

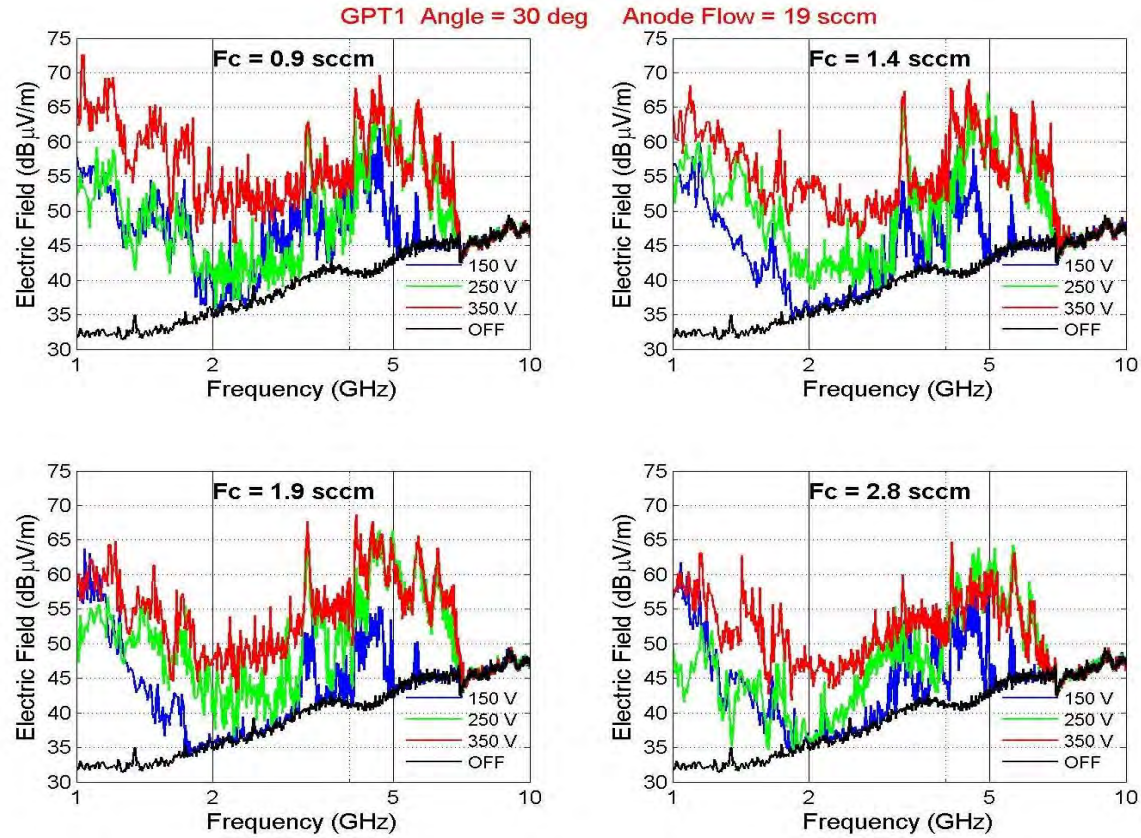

Figure 4. 1-10 GHz emission for an anode flow rate of 19 sccm, 4 cathode flow rates, and 3 discharge voltages. Magnetic field varied with discharge voltage. The black line is the background emission (thruster unpowered).

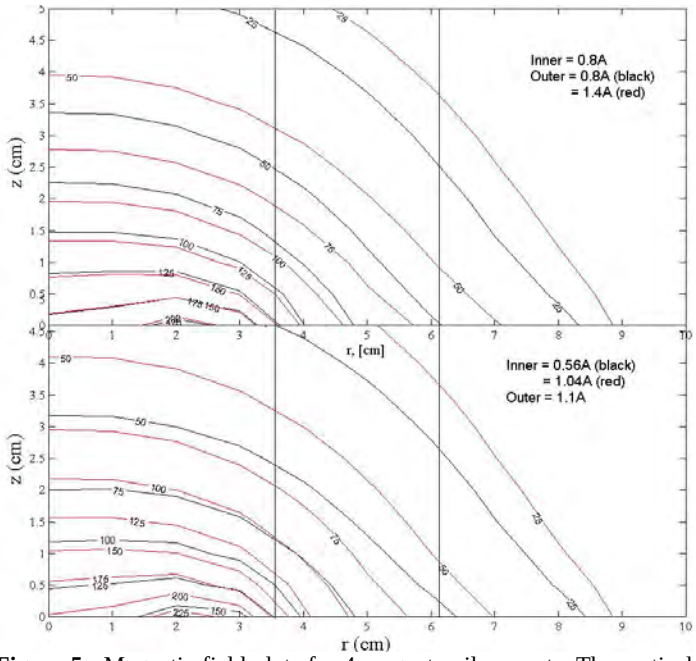

Figure 5. Magnetic field plots for 4 magnet coil currents. The vertical axis is distance from thruster face; horizontal axis is distance from thruster centerline. Two vertical lines mark the position of thruster channel. Cathode orifice is at r = 10 cm, z = 0 cm.

Based on these results and the information that another principal difference between the SPT-100 and PPS©1350 Hall thrusters is their magnetic field profiles[13] we pursued a study of emission as a function of magnetic field strength. The magnetic field is varied by adjusting the current in the inner and outer coils shown in Figure 1a. Figure 5 displays contour maps of the magnetic field for the four extreme cases studied. These were taken by translating the probe of a magnetometer in the region outside the channel of the non-operating thruster. Magnetic field plots (for example, see figure 1c) indicate that the flux lines are orthogonal to the contour lines shown in Figure 5. The upper plot in this figure shows the effect of varying the outer coil current and the lower plot of varying the inner coil current. The position of the cathode orifice is at the lower right corner of each plot.

Varying the current in either coil has similar effects. The high and low field contours are remarkably similar just outside the channel for both plots. However, the field values near the inner wall of the channel increase as much as 50 G at a given location when increasing the inner current from 0.56 to 1.04 A; the field increase is about half this amount when increasing the outer current from 0.8 to 1.4 A. in this region. The field gradients nearly double near the inner channel wall for the change in the inner coil current but do not significantly change when increasing the outer coil current. Extrapolating the values shown, one expects a field of < 10 G at the cathode orifice and a change of < 5 G for the currents shown. Near the cathode, the field gradient is < 15G/cm for all four magnetic configurations.

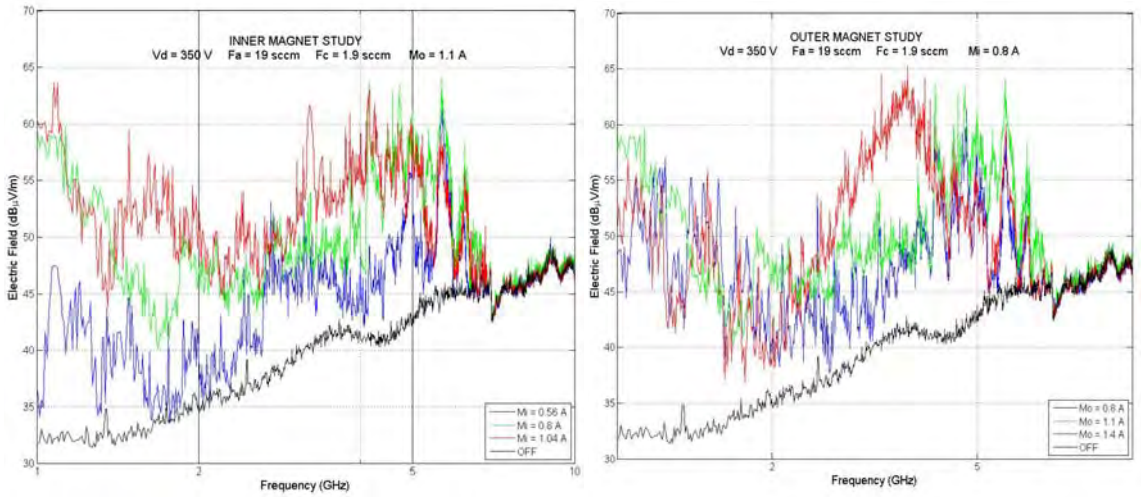

Figure 6. Spectra for differing values of the magnetic field. The left panel shows 3 spectra holding the outer magnet coil current at 1.1 A while increasing the inner coil current from 0.56 A to 1.04 A. The right panel shows 3 spectra where the outer coil current is varied from 0.8 A to 1.4 A while holding the inner coil current at 0.8A.

The emission in the 1 – 10 GHz range as a function of magnetic field is shown in Figure 6. Here the anode flow rate of 19 sccm and 350 V discharge voltage were used (thruster modes 25-29 in Table 1). It is clear from these data that increasing the magnetic field using either the inner or outer magnet coils increases the emission. The emission in the L-band appears to be sensitive to a change in the inner coil magnet, whereas

the radiated electric field can be seen to increase an order of magnitude (20 dB) as the magnetic field increases. Other plots at different field strengths confirm this L-band sensitivity. The outer magnet study shown on the rights does not show this degree of sensitivity. Both the inner and outer coil studies show comparable sensitivity to the emission in the S and C bands.

Time Domain Measurements

A series of time domain measurements were taken using an antenna, Low noise amplifier (LNA), and a fast digitizing sampling oscilloscope (DSO). Specifically, no envelope detector was used thus allowing the RF waveform to be observed given an oscilloscope with sufficient bandwidth. Data were taken with two different DSOs; one with a 3 GHz bandwidth and later with DSO with a 15 GHz bandwidth. A small fraction of the data taken with the 3 GHz bandwidth DSO will be presented here to indicate the time-resolved character of the emission and to show some of the shortcomings of the spectral data. A complete analysis of these data will be presented in a future publication.

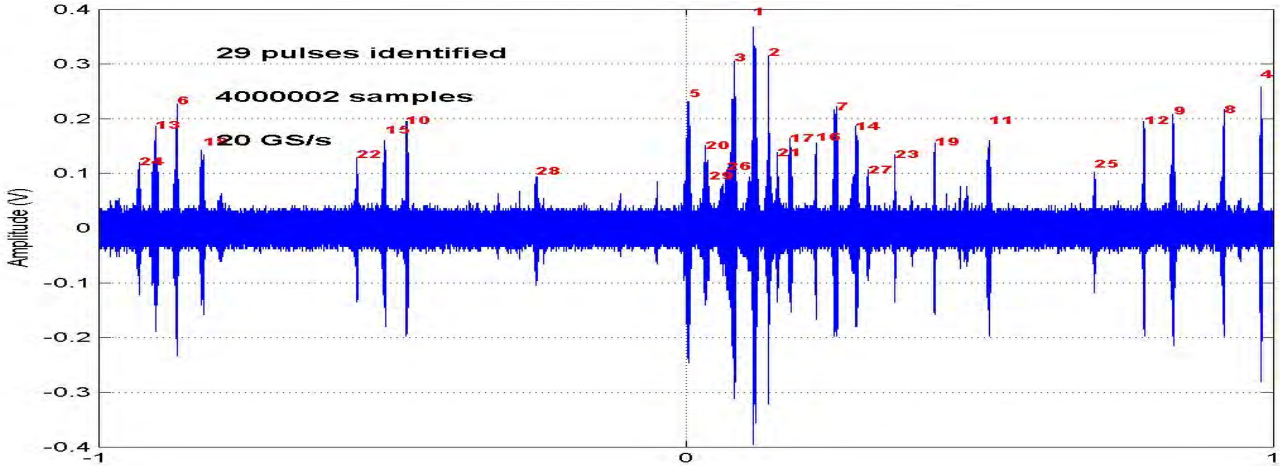

Figure 7. A 200-μs trace showing the individual pulses emitted from a Hall thruster in L-band.

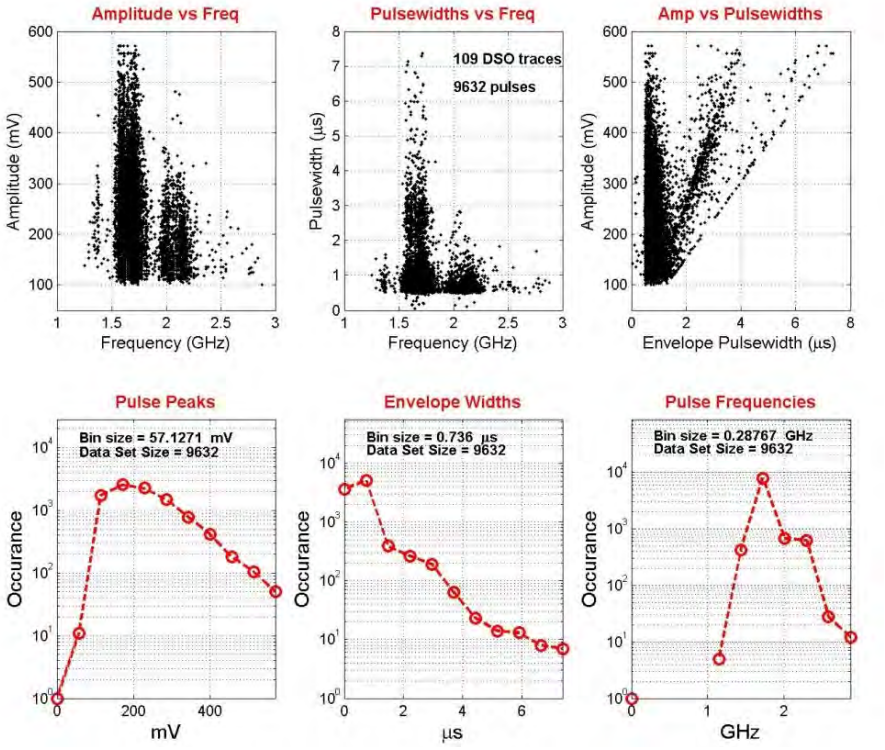

Figure 8. Analysis of 109 traces of the type shown in Figure 7. These plots display the characteristics of the individual pulses (upper three plots) and their statistical properties (lower three plots).

Figure 7 shows one 4 mega-sample trace at 20 GS/s sampling rate from a 3 GHz bandwidth DSO. This trace was acquired with the thruster operating in mode 26 of Table 1. There are 29 pulses identified in the L-band in this 200-μs trace. Expanding any pulse will reveal the RF waveform and this waveform can be Fourier analyzed for its frequency components. This technique has the potential to identify the frequency components in each pulse in contrast to data taken with an envelope detector placed in the signal train.

With the proper software, each pulse can be analyzed for amplitude, pulse width, and frequency. An example of this analysis is given in Figure 8. Here 109 single sweep oscilloscope traces of the form shown in Figure 7 were examined. The upper three panels of this figure display plots characteristics of individual pulses whereas the lower three panels display statistical analysis presented as histograms of the same data. In viewing these data it is important to remember that the combination of the antenna and DSO bandwidths limit the frequency window to 1-3 GHz and the data have not been corrected for the variation in sensitivity of the antenna which decreases by 14% with increasing frequency over this frequency interval (the LNA response is flat).

From these data the pulsed nature of the emission in the L-band is obvious, a fundamental property that is not apparent from the spectral data. Based on data not shown here, these pulses can be emitted in groups whose separation is typically 100-200 microseconds. The characteristics of this grouping are a function of thruster operating mode and in particular the cathode xenon flow rate.

Examination of the frequency components of individual pulses (not shown) indicate that most pulses are sharply peaked around a single frequency. Assigning this frequency to individual pulses allowed the frequency plots in Figure 8 to be made. Note that, within this narrow frequency range, the pulses occur principally at two frequencies with many fewer pulses at frequencies clustered at a frequency below and (possibly) above these two frequencies. Note too that the pulse widths range from a few pulses near 100 ns to above 5 μs, with the majority between 1 and 3 μs with a peaked occurrence near 500 ns. There seems to be no simple relationship between pulse width and pulse frequency (center plot of Fig. 8). For most pulses, there seems to be little relationship between pulse amplitude and pulse width but for some there is a linear relationship with two different slopes (right plot of Fig. 8).

IV. Conclusions and Discussion

The spectral studies indicate that changes in cathode angle do not significantly alter the radiated electric field in the L, S, and C-bands. The same is true for variations in the cathode flow rate with the exception of the sensitivity of the L-band emission to a cathode operating in a xenon starved condition. In contrast, the emission in these bands proves to be quite sensitive to changes in magnetic field where increasing the magnetic field increases the emission and an inverse relationship between discharge voltage and emission when the magnetic field is held constant. Interestingly, the L-band emission was more sensitive to changes in the magnetic field near the inner channel wall. Previous studies[8] indicate that this emission originates near the cathode where the changes in the magnetic field were least. Our understanding the correlation between the magnetic field changes and the emissions is incomplete.

It is clear that time domain measurements for emission of this type offer more detailed information than frequency domain measurements. The spectral scans are taken with a peak-and-hold detector, dwelling on a frequency with a specified bandwidth for a specified time interval retaining only the highest amplitude pulse during the interval before stepping to the next frequency. For EMC measurements the dwell time is chosen to record worst case scenarios. Consequently, the spectral scans can be misleading as to the relative importance of emission. For example, if a maximum amplitude pulse at one frequency occurs once per dwell interval it will look exactly the same on a spectral plot as an equal magnitude pulse occurring 1000 times during the same interval at another frequency. Statistical analysis of time domain data of the type presented here can overcome this misperception.

The discovery of the physical origin of the emission from Hall thrusters will be aided by detail information on the characteristics of the emission that will likely come from the time domain data. To this end, we are collecting simultaneous data in bands (UHF, L, S, and C) to understand correlations across the bands on a pulse-by-pulse basis. This radiated emission combined with high frequency probe data of the type presented in reference 8 will lead to further physical insights.

Acknowledgements

This work was supported by The Aerospace Corporation's Independent Research and Development Program.

V. References

1. E. Y. Choueiri, "Plasma Oscillations in Hall Thrusters," Phys. Plasmas **8**(4), 1411–1426 (2001).

2. E.J. Beiting, J.E Pollard, V. Khayms, and L. Werthman, IEPC-03-129, Toulouse, 17-21 March 2003.

3. V. I. Brukhty and K. O. Kirdyashev," IEPC99-107, (IEPC), Kitakyushu, Japan, 17-21 October 1999.

4. K. P. Kirdyashev, "Electromagnetic Interference with Hall Thruster Operation," EAS SP-555, 4th ISPC, Cagliari, Sardinia, Italy, 2-4 June 2004

5. E. J. Beiting, M. L. Garrett, and J. E. Pollard, AIAA-2006-5262, Sacramento, CA, 9-12 July 2006

6. E. J. Beiting, M. L. Garrett, J. E. Pollard, B. Pezet, and P. Gouvernayre, IEPC-2005-221, Princeton, NJ, 2005.

7. E. J. Beiting, M. L. Garrett, J. E. Pollard, B. Pezet, and P. Gouvernayre, IEPC-2005-222, Princeton, NJ, 2005

8. E. J. Beiting, R. Spektor, M. L. Garrett, ISPC-2008-070, Crete, Greece 2008.

9. E. J. Beiting, X. L. Eapen, J. E. Pollard, M. Gambon, F.R. Marchandise, and M. Oberg, IEPC-2009-71, Ann Arbor, MI, USA, 2009.

10. E. J. Beiting and M. L Garrett, AIAA-2007-5329, Cincinnati, OH, July 8-11, 2007.

11. Y. Raitses, D. Staack, M. Keidar, and N. J. Fisch, "Electron-wall interaction in Hall thrusters," Phys. Plasmas **12**(057104) (2005).

12. Y. Raitses, D. Staack, D. Dunaevsky, and N. J. Fisch, "Operation of a Segmented Hall Thruster with Lowsputtering Carbon-velvet Electrodes," J. Appl. Phys **99** (036103) (2006).

13. F.R. Marchandise and M. Oberg, personal communication, 2009.